Proc. Natl. Acad. Sci. USA
Vol. 94, pp. 6432–6437, June 1997
Medical Sciences

Intercellular adhesion molecule 1 knockout abrogates radiation induced pulmonary inflammation

(ionizing radiation/lung/inflammation/knockout mice)

DENNIS E. HALLAHAN* AND SUBBULAKSHMI VIRUDACHALAM

Department of Radiation and Cellular Oncology, University of Chicago and Pritzker School of Medicine, Chicago, IL 60637

Communicated by Donald F. Steiner, University of Chicago, Chicago, IL, March 20, 1997 (received for review December 2, 1996)

ABSTRACT **Increased expression of intercellular adhesion molecule 1 (ICAM-1; CD54) is induced by exposure to ionizing radiation. The lung was used as a model to study the role of ICAM-1 in the pathogenesis of the radiation-induced inflammation-like response. ICAM-1 expression increased in the pulmonary microvascular endothelium and not in the endothelium of larger pulmonary vessels following treatment of mice with thoracic irradiation. To quantify radiation-induced ICAM-1 expression, we utilized fluorescence-activated cell sorting analysis of anti-ICAM-1 antibody labeling of pulmonary microvascular endothelial cells from human cadaver donors (HMVEC-L cells). Fluorochrome conjugates and UV microscopy were used to quantify the fluorescence intensity of ICAM in the irradiated lung. These studies showed a dose- and time-dependent increase in ICAM-1 expression in the pulmonary microvascular endothelium. Peak expression occurred at 24 h, while threshold dose was as low as 2 Gy. To determine whether ICAM-1 is required for inflammatory cell infiltration into the irradiated lung, the anti-ICAM-1 blocking antibody was administered by tail vein injection to mice following thoracic irradiation. Inflammatory cells were quantified by immunofluorescence for leukocyte common antigen (CD45). Mice treated with the anti-ICAM-1 blocking antibody showed attenuation of inflammatory cell infiltration into the lung in response to ionizing radiation exposure. To verify the requirement of ICAM-1 in the inflammation-like radiation response, we utilized the ICAM-1 knockout mouse. ICAM-1 was not expressed in the lungs of ICAM-1-deficient mice following treatment with thoracic irradiation. ICAM-1 knockout mice had no increase in the inflammatory cell infiltration into the lung in response to thoracic irradiation. These studies demonstrate a radiation dose-dependent increase in ICAM-1 expression in the pulmonary microvascular endothelium, and show that ICAM-1 is required for inflammatory cell infiltration into the irradiated lung.**

Leukocyte accumulation at sites of tissue injury requires the combined action of multiple families of cell adhesion molecules (reviewed in refs. 1 and 2). Adhesion of leukocytes to the vascular endothelium is an essential step in the inflammatory cell emigration from the circulation (3). The adhesion event is mediated by the interaction of molecules present on the surface of both endothelial cells and inflammatory cells (4). The intercellular adhesion molecule 1 (ICAM-1; CD54) is expressed on vascular endothelial cells and is a counter-receptor for integrins in leukocytes, including CD11b/CD18 (Mac-1), and CD11a/CD18 (LFA-1) (reviewed in refs. 1 and 2). This interaction between ICAM-1 and integrins on leukocytes promotes adhesion and transendothelial migration of leukocytes (5). The requirement for ICAM-1 during leukocyte recruitment to sites of inflammation and tissue injury have been demonstrated in studies using monoclonal anti-ICAM-1 antibodies to block the interaction between integrins on inflammatory cells and endothelial adhesion molecules (6, 7). The requirement for ICAM-1 in the recruitment of inflammatory cells has been further demonstrated in ICAM-1-deficient mice (8). These ICAM-$1^{-/-}$ mice do not develop inflammation in response to cytokine challenge.

Recent studies have shown that ICAM-1 expression is induced by ionizing radiation (9, 10). Radiation-mediated ICAM-1 expression is required for leukocyte adhesion to irradiated endothelial cells in culture (10). Ionizing radiation has long been recognized to induce an inflammation-like response within irradiated tissues (11–14). In particular, the lung is especially intolerant of ionizing radiation. Inflammation is the predominant early histologic change within the irradiated lung (15–20). Histologic sections and bronchoalveolar lavage of the irradiated lung have demonstrated a time- and dose-dependent inflammatory response (19, 21–23). The sensitivity of particular strains of mice to ionizing radiation is associated with the predisposition to a development of pulmonary inflammation (radiation pneumonitis). Foci of inflammation are regions of tissue injury within the irradiated lung (24). The lung was therefore utilized as a model to determine the role of ICAM-1 in the pathogenesis of radiation-induced tissue injury in the present study.

Studies presented here demonstrated that ICAM-1 expression was induced within the pulmonary capillary endothelium after exposure to thoracic irradiation. We found a dose-dependent increase and ICAM-1 expression in primary cultures of human pulmonary microvascular endothelial cells cultured from cadaver lungs. To determine whether ICAM-1 expression is required for radiation-mediated inflammatory changes in the lung, we utilized ICAM-1 blocking antibodies and the ICAM-1 knockout mouse. These studies demonstrated that there was a radiation dose-dependent increase in ICAM-1 expression within pulmonary microvascular endothelium and that ICAM-1 is required for inflammatory cell infiltration into in the irradiated lung.

METHODS

ICAM-1 Quantitation on Human Pulmonary Microvascular Endothelial Cells. Human microvessel endothelial cells (HMVEC-L; Clonetics, San Diego) were grown in EGM (Clonetics) medium with 10% fetal bovine serum. Endothelial cells were grown to 80% confluence and irradiated with a GE Maxitron x-ray generator as described (10, 25). Cells were

The publication costs of this article were defrayed in part by page charge payment. This article must therefore be hereby marked "*advertisement*" in accordance with 18 U.S.C. §1734 solely to indicate this fact.

Abbreviations: ICAM-1, intercellular adhesion molecule 1; HMVEC-L, human microvessel endothelial cells; FITC, fluorescein isothiocyanate; IL, interleukin; HRP, horseradish peroxidase; DAPI, 4′,6-diamidino-2-phenylindole.

*To whom reprint requests should be addressed at: Department of Radiation Oncology, MC 0085, 5841 South Maryland, University of Chicago, Chicago, IL 60637.

removed from flasks with 0.1% collagenase, 0.01% EDTA, and 0.25% BSA and pelleted in polystyrene tubes. Cells were then incubated with primary IgG1 antibody (mouse antihuman ICAM-1; R & D Systems) for 20 min at 4°C. The cells were then rinsed with isotonic PBS, pelleted, and incubated with fluorescein isothiocyanate (FITC)-conjugated secondary antibody (goat anti-mouse IgG1) for 20 min at 4°C. The fluorescein-labeled cells were rinsed in PBS and fixed in PBS containing 0.01% paraformaldehyde. Nonspecific binding was evaluated with the use of FITC-conjugated secondary antibody alone and with a lymphocyte-specific first-step antibody, anti-CD_{10}, which does not bind to endothelial cells.

Fluorescence-activated cell sorting analysis was utilized for quantification of receptor expression of ICAM on HMVEC-L as previously described (10). The Becton Dickinson FACScan was used with LYSIS II software. Forward and side scatter fluorescence data identified 10,000 viable endothelial cells in each experimental group for unlabeled cells, nonspecific-antibody-labeled cells, and anti-CAM-antibody-labeled cells. Fluorescence data were then accumulated on each group of 10,000 cells at 530 nm, the wavelength emitted by FITC after treatment with x-rays or interleukin 1 (IL-1) (10 ng/ml; R & D Systems). These fluorescence data were expressed as histograms of events versus log fluorescence and analyzed in comparison to the autofluorescence of unlabeled cells as well as the fluorescence of baseline or anti-CAM-labeled cells as appropriate. The percentage of cells synthesizing adhesion molecules was determined by quantification of the number of cells demonstrating an increase in log fluorescence beyond that of untreated control cells.

Thoracic Irradiation. Mice were treated with thoracic irradiation at 12.75 Gy. This dose was selected because it induces radiation pneumonitis that results in lethality in 50% of mice within 180 days ($LD_{50/180}$). Six, 24, and 48 h after irradiation, mice were euthanized by intraperitoneal injection of barbiturate. Lungs were fixed in formalin and embedded in paraffin. Paraffin blocks were then sectioned (5 μm thick) and placed on slides. In separate experiments mice were treated with thoracic irradiation and lungs were dissected and fixed at 35 days. Paraffin blocks were sectioned and stained with rat anti-mouse CD45 (leukocyte common antigen; PharMingen). CD45 staining cells in ten ×40 microscopic fields were counted from each of three mice, and the means and standard errors were calculated.

Immunohistochemistry. Sections (5 μm) of each lung were mounted onto Superfrost Plus slides (Fisher Scientific) baked at 60°C for 1 h, cleared in xylene, and hydrated through a descending alcohol series to distilled water. For E-selectin and CD45 immunostaining, the hydrated sections were incubated with Protease I (Ventana Biotech, Tucson, AZ) for 8 min at 42°C. For ICAM immunostaining, the hydrated sections were incubated with Protease II (Ventana Biotech) for 8 min at 42°C. After washing briefly in ddH_2O, endogenous activity was blocked by treatment of the sections with 3% hydrogen peroxide in methanol for 20 min. Two tissue sections from each case were then incubated overnight at 4°C at a titer of 2.5 μg/ml for CD45 and ICAM (PharMingen). One slide from each sample was treated in a similar fashion and incubated overnight in normal serum immunoglobulin (Ventana Medical Systems, Tucson, AZ). The immunohistochemical staining was performed on a Ventana Gen[11] system (Ventana Medical Systems). The Ventana Gen[11] utilizes an indirect strepavidin biotin system conjugated with horseradish peroxidase (HRP) for detecting the immunocomplex and diaminobenzidine as substrate for localization. The Ventana Gen[11] uses a cartridge delivered avidin/biotin blocking kit to block endogenous biotin. The immunostained sections were counterstained with hematoxylin, dehydrated through an ascending alcohol series, cleared, and coverslipped.

During antibody-blocking studies, C3H mice were treated with thoracic irradiation (12.75 Gy). A single injection of 50 μg of the ICAM-1-blocking antibody (Becton Dickinson) was administered by tail vein injection at 16 h after irradiation. Lungs were dissected and fixed in formalin at 35 days. Paraffin blocks were sectioned and stained using rat anti-mouse CD45. Again, ten ×40 microscopic fields were counted from each of three mice, and the means and standard errors were calculated.

Immunofluorescence Staining. Immunofluorescence replaced HRP immunohistochemistry when quantitation was needed because fluorescence intensity can be measured. Lung sections (5 μm) were mounted on slides and labeled with antibodies (ICAM-1 or CD45) as described above. Following incubation with biotinylated secondary antibody, blocking solution was added for 30 min in a humid chamber at 37°C. Avidin-Cy3 (5 μg/ml; Amersham) was added to 200 μl of blocking buffer and filtered through a 0.2-μm Millipore filter. Avidin-Cy3 solution was added to tissue sections, coverslipped and incubated for 30 min in a humid chamber at 37°C. Coverslips were removed and sections were washed using 4× standard saline citrate (SSC)/0.1% Triton X-100 at 39°C. Slides were counterstained in 4′,6-diamidino-2-phenylindole (DAPI) and rinsed with 2× SSC for 10 sec. Slides were then coverslipped with antifade and blotted. Immunofluorescence was visualized using UV microscopy and NIH IMAGE software as described (26). CY3-labeled CD45+ cells were counted in ten ×40 microscopic fields. The mean and SEM were calculated.

During quantitation of ICAM-1 *in vivo*, immunofluorescence was visualized using UV microscopy, NU200 and NIH IMAGE software. DAPI staining of nuclei was used as a control to verify that fluorescence was measured in the same number of cells in each lung section. Fifty nuclei were framed and anti-ICAM immunofluorescence was determined by use of NIH IMAGE software. Fluorescence intensity was determined for each pixel within the framed cells and the number of fluorescent pixels were counted by use of NIH IMAGE. The increase in the number of pixels showing fluorescence was determined. The mean and SEM of anti-ICAM-1 immunofluorescence of three lungs was determined for each dose of thoracic irradiation.

Irradiation of ICAM-1-Deficient Mice. ICAM-1-deficient ($ICAM\text{-}1^{-/-}$) mice (8) were obtained from The Jackson Laboratories and were crossbred with $ICAM\text{-}1^{+/+}$ mice in the University of Chicago Transgenic core laboratory to obtain $ICAM^{+/-}$ progeny. The $ICAM^{-/-}$ mice were developed from C57BL/6 mice which develop inflammatory cell infiltrates within the irradiated lung (24). $ICAM\text{-}1^{+/+}$, $ICAM\text{-}1^{-/-}$, and heterozygous mice were each treated in the following manner during the same experiment: 6-week-old mice were treated with thoracic irradiation using 12.75 Gy. At 1, 2, and 35 days following irradiation, mice were euthanized with i.p. phenobarbital. Lungs were dissected and fixed in formalin. Paraffin blocks were sectioned and stained as described above. Paraffin sections of lungs were stained with rat anti-mouse ICAM-1 (R & D Systems) or rat anti-mouse CD45 (leukocyte common antigen) as described above. CD45-stained cells were counted as described above.

RESULTS

Quantitation of ICAM-1 Expression on HMVEC-L Cells. To characterize the pattern of ICAM-1 expression in irradiated endothelial cells, we irradiated HMVEC-L endothelial cells from cadaver donors (Clonetics). The HMVEC-L cells were irradiated with 1, 2, 5, 10, and 20 Gy. At 1, 24, 48, and 72 h following irradiation, cells were fixed and stained with anti-ICAM-1 antibody. Fig. 1 shows a dose-dependent increase at 24 h and the percentage of endothelial expressing ICAM-1 at 24 h after x-irradiation. There was no increase in ICAM

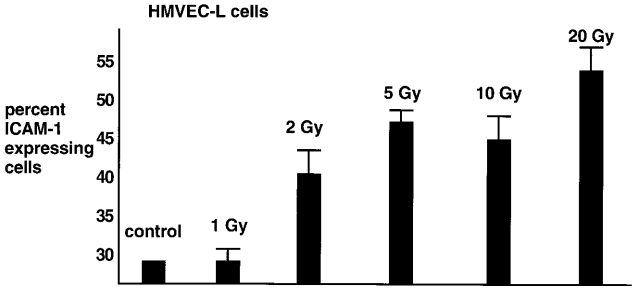

FIG. 1. ICAM-1 expression on HMVEC-L endothelial cells. Cells were treated with the indicated radiation doses. At 24 h after irradiation, cells were fixed and labeled with anti-ICAM-1 antibody and FITC-conjugated secondary antibody. Fluorescence-activated cell sorting analysis was used to quantify the number of endothelial cells expressing ICAM-1. Shown are the mean and standard error of the mean from three experiments.

expression at 1 h, whereas expression persisted to 72 h after radiation. There was no increase in ICAM-1 expression after exposure to 1 Gy. A dose-dependent increase in the percentage of endothelial cells expressing ICAM-1 was observed beginning at 2 Gy (40%, $P = 0.06$), and increased to 53% of cells after exposure to 20 Gy ($P = 0.01$).

Cell Adhesion Molecule Expression on Pulmonary Vascular Endothelium of Mice Treated with Thoracic Irradiation. To study expression of ICAM-1 protein *in vivo* in the lung, we irradiated the thorax of C3H mice. Six, 24, and 48 h and 7 days after irradiation, mice were euthanized by i.p. injection of barbiturate and lungs were fixed and sectioned. Lung sections were incubated with rat anti-mouse ICAM-1 (R & D Systems). Low levels of ICAM-1 expression were found in the pulmonary vascular endothelium of untreated mice (Fig. 2). ICAM expression increased at 24 h after irradiation and persisted for 7 days after irradiation (Fig. 3). The predominant pattern of staining was in the microvascular endothelium within the alveolar septa.

To quantify ICAM-1 expression *in vivo*, immunofluorescence was visualized using UV microscopy and NIH IMAGE software. DAPI staining of nuclei were used as to verify that fluorescence was calculated for the same number of cells in each lung section. Fifty nuclei were framed and anti-ICAM immunofluorescence was determined by use of NIH IMAGE software (Fig. 2*A*). The fold increase in the number of pixels showing fluorescence was determined. Shown in Fig. 2*B* are the mean and SEM of the fold increase in fluorescence for each dose of thoracic irradiation. We found that a dose of 2 Gy increased anti-ICAM immunofluorescence by 50%, while a dose of 5 Gy increased expression 3-fold and 10 Gy produced a 5-fold increase as compared with anti-ICAM immunofluorescence in untreated control lungs (Fig. 2*B*).

Inflammatory Cell Infiltration into the Irradiated Lung. To characterize leukocyte infiltration into the lungs of C3H mice treated with thoracic irradiation, lungs were fixed and sectioned 35 days after exposure to 12.75 Gy of radiation. Lung sections were incubated with antibody to murine leukocyte common antigen (CD45). Fig. 4 shows minimal leukocyte staining in lungs from mice treated with sham irradiation and an increase in leukocyte staining within the alveoli and septa of mice at 35 days after thoracic irradiation. To determine whether ICAM-1 is required for infiltration of leukocytes into the irradiated lung, we injected the anti-ICAM-1 blocking antibody by tail vein injection at 16 h after irradiation. This antibody has been shown to block leukocyte binding to irradiated endothelial cells (10). The lungs from irradiated C3H mice treated with the anti-ICAM-1-blocking antibody showed attenuated leukocyte staining at 35 days as compared with animals injected with pre-immune antiserum (Fig. 4*C*). Table 1 shows the quantification of CD45-stained cells in lungs of

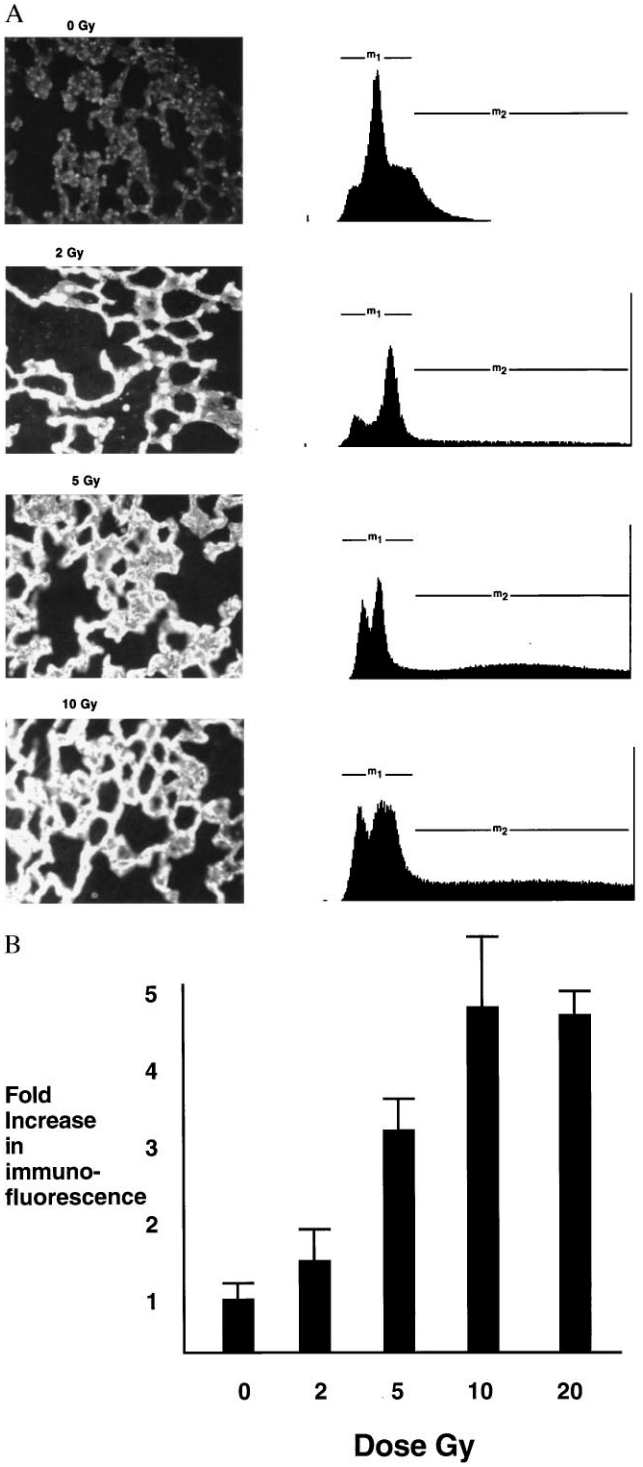

FIG. 2. (*A*) Anti-ICAM-1 immunofluorescence staining in the irradiated lung. C3H mice were treated with the indicated doses of thoracic irradiation (0, 2, 5, and 10 Gy) and lungs were sectioned at 24 h after irradiation. Sections were incubated with biotinylated antibody followed by avidin-Cy3 fluorochrome. Fluorescence was imaged by UV microscopy and NIH IMAGE software. The intensity of fluorescence was then measured for each pixel and graphed as number of pixels at each level of brightness. (*B*) Bar graph showing the mean and SEM of the fold-increase in anti-ICAM-1 immuno-fluorescence staining in the irradiated lung following the indicated doses.

C3H mice treated with thoracic irradiation. CD45-stained cells were counted in ten ×40 power fields and the average number of leukocytes per field is shown. The average number of inflammatory cells in lungs from control mice was 16 per ×40

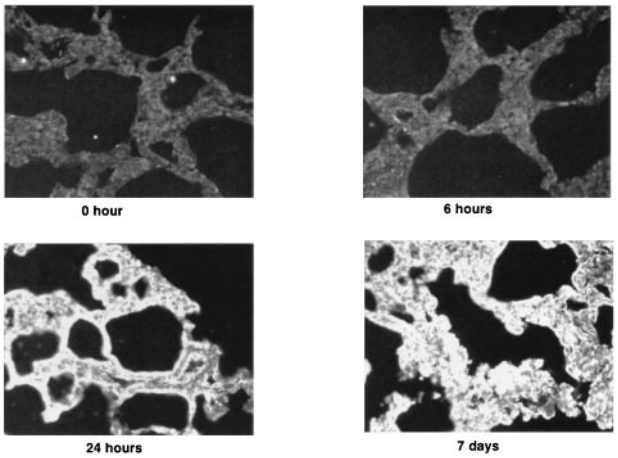

FIG. 3. Time-dependent increase in immunofluorescence staining for ICAM-1 in the irradiated lung. Mice were treated with 10 Gy thoracic irradiation and lungs were fixed at the indicated times.

field, whereas the inflammatory cell count in lungs from mice treated with thoracic irradiation was 55 per ×40 field ($P <$ 0.01). Mice receiving anti-ICAM-1-blocking antibody after thoracic irradiation had 23 CD45 cells/field as compared with 12 CD45 cells/field in lungs from mice treated with antibody and no irradiation (Table 1).

Radiation-Mediated Inflammation in ICAM-1-Deficient Mice. To substantiate the role of ICAM-1 in the pathogenesis of radiation-mediated inflammation, we studied microscopic sections of lungs from x-irradiated ICAM-$1^{-/-}$ mice. ICAM-$1^{-/-}$ mice were crossbred with $ICAM^{+/+}$ mice to determine whether ionizing radiation induces inflammatory cell infiltration into lungs of $ICAM^{+/+}$, $ICAM^{-/-}$, and $ICAM^{+/-}$ mice. Mice were treated with thoracic irradiation or sham irradiation. The lungs were excised at 24 and 48 h after irradiation, sectioned, and stained with the anti-ICAM-1 antibody. As shown in Fig. 5, ICAM-1 expression in the pulmonary vascular endothelium was not detected in ICAM-1-deficient mice. Radiation-mediated ICAM expression was attenuated in $ICAM^{+/-}$ mice (Fig. 5). In contrast, $ICAM^{+/+}$ mice had a marked increase in ICAM-1 expression following thoracic irradiation.

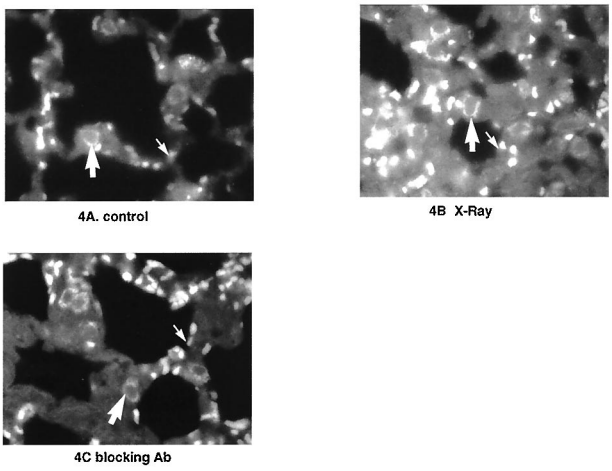

FIG. 4. Immunohistochemical staining for leukocyte common antigen (CD45) in the lungs from C3H mice treated with (*A*) sham irradiation, (*B*) x-irradiation, or (*C*) x-irradiation followed by ICAM-1 blocking antibody. Five weeks after treatment, lungs were fixed, sectioned, and stained with anti-CD45 antibody using HRP conjugates. Large arrows indicate CD45 on inflammatory cells, and small arrows indicate erythrocytes which demonstrate autofluorescence.

Table 1. Average numbers of CD45-staining cells within the lungs of C3H mice (leukocytes per ×40 field)

	Control	Preimmune antiserum	Anti-ICAM-1 antibody
Irradiated	55	49	23*
Nonirradiated	16	14	12

*$P < 0.05$ as compared to irradiated mice receiving preimmune antiserum.

To determine whether ICAM is required for radiation-mediated inflammation, we studied inflammatory cell infiltration into the lungs of irradiated ICAM-deficient mice. Immunofluorescence of anti-CD45 antibody was used to label and count inflammatory cells in lung sections. ICAM-$1^{-/-}$ mice (8) were treated with thoracic irradiation and lungs were dissected at 5 weeks after irradiation. Table 2 shows the average number of CD45 staining cells from ten ×40 fields. Fig. 6 shows inflammatory cells labeled with CD45 antibody immunofluorescence in lung sections. Irradiated lungs from $ICAM^{+/+}$ mice had a mean of 43 CD45 staining cells per ×40 field, as compared with 18 CD45 staining cells per ×40 field in nonirradiated lungs ($P < 0.05$). In contrast, lungs from ICAM-1-deficient mice had 5 CD45 staining cells per ×40 field following irradiation, as compared with 4 CD45 staining cells per ×40 field in lungs from nonirradiated control mice (Table 2). Inflammatory cell infiltration into irradiated lungs of $ICAM^{+/-}$ mice (32 per ×40 field) approximated that in $ICAM^{+/+}$ mice ($P > 0.1$), indicating that reduced ICAM-1 expression is not sufficient to prevent radiation pneumonitis.

DISCUSSION

Our objective in this study was to characterize the radiation-mediated induction of ICAM-1 in the irradiated lung. The initial time of ICAM-1 expression on irradiated endothelial cells in culture is similar to that observed in the pulmonary vascular endothelial cells of mice treated with thoracic irradiation (10). ICAM-1 expression on endothelial cells begins at 24 h and persists for 7 days. The single dose required to achieve ICAM-1 expression in the irradiated lung is greater than 2 Gy in the present study. A dose of 2 Gy is typically used during radiation therapy. The risk of radiation pneumonitis increases with increasing fraction size (reviewed in refs. 27 and 28). When patients are treated with a 10-Gy dose during total body radiation, this gives an increased incidence of radiation pneumonitis as compared with 13.5 Gy given as 1.5-Gy fractions twice daily. Fraction sizes greater than or equal to 2.5 Gy gave a greater incidence of radiation pneumonitis. We propose that ICAM-1 induction and the consequent inflammatory infiltration into the lung in part contributes to the dose-dependent incidence of radiation pneumonitis.

Immunofluorescence was used to study ICAM expression in the lungs of irradiated mice. This technique is semiquantitative, because immunofluorescence may be amplified by this

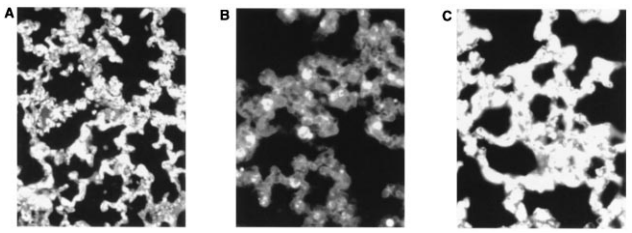

FIG. 5. Immunohistochemical staining for ICAM-1 in the lungs from irradiated C57bl6/B6 (*A*) $ICAM^{+/-}$ mice, (*B*) $ICAM^{-/-}$ mice, and (*C*) $ICAM^{+/+}$ mice. Mice were treated with thoracic irradiation and lungs were fixed 48 h after treatment. Lung sections were stained with anti-ICAM-1 antibody using HRP conjugates.

Table 2. Average numbers of CD45-staining cells in the lungs of ICAM-1-deficient and ICAM$^{+/+}$ mice (leukocytes per ×40 field)

	ICAM-1$^{+/+}$	ICAM-1$^{-/-}$	ICAM-1$^{+/-}$
Irradiated	43	5*	32
Nonirradiated	18	4	14

*$P < 0.01$.

technique. Three layers of staining are used. Anti-CD45 antibody is the first layer. Multiple biotinylated secondary antibodies may bind to each of the primary antibodies. Multiple avidin-fluorochrome molecules will then bind to each of these secondary antibodies. The net effect is amplification of the fluorescence of anti-ICAM antibody. Therefore, we expect that quantification of the fluorescence by use of this system may be an overestimate of ICAM expression *in vivo*.

Ionizing radiation mediates adhesion of leukocytes to endothelial cells. We and others have demonstrated that neutrophils bind to irradiated endothelial cells *in vitro* (10, 29–31). ICAM-1-blocking antibodies effectively prevented leukocyte adhesion to irradiated endothelial cells. To determine whether blocking antibodies also prevent leukocyte infiltration into the irradiated lung, we administered the monoclonal anti-ICAM-1 antibody to mice following thoracic irradiation. Anti-ICAM-1 antibody attenuated the increase and the number of CD45 staining cells within the lungs of irradiated mice. The effectiveness of a single administration of the blocking antibody suggests that radiation-mediated ICAM-1 induction is transient, as we have described (10). The requirement of ICAM-1 expression in the development of inflammatory cell infiltration in the irradiated lung was verified by the use of ICAM-1-deficient mice. We found that ICAM-1$^{-/-}$ mice did not develop an increase in CD45 staining cells in the lung following thoracic irradiation.

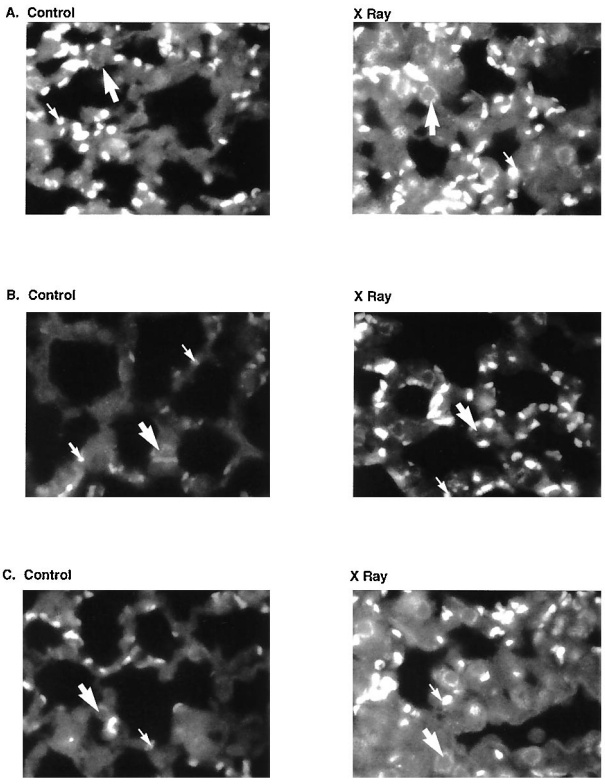

FIG. 6. Immunofluorescent staining for inflammatory cell infiltration by use of anti-CD45 in nonirradiated control and irradiated lungs from (*A*) ICAM$^{+/+}$ mice, (*B*) ICAM$^{-/-}$ mice, and (*C*) ICAM$^{+/-}$ mice. Five weeks after treatment, lungs were fixed, sectioned, and stained with anti-CD45 antibody using rhodamine conjugates. Shown are photomicrographs of UV microscopy. Large arrows indicate CD45 on inflammatory cells, and small arrows indicate erythrocytes which demonstrate autofluorescence.

To quantify the number of inflammatory cells in the irradiated lung, we utilized antibodies to leukocyte common antigen (CD45), which is present on all leukocytes. CD45-stained cells were then counted under ×40 objective microscopic analysis. HRP-conjugated antibodies gave the same cell count as fluorochrome-conjugated antibody. We show photographs of CY3 fluorochrome rather than HRP, because it gives greater intensity and contrast during imaging, and the black and white photographs are more easily interpreted. The number of CD45-stained cells shown in Fig. 6 is less than the cell count shown in Table 2 for two reasons. The captured image is ≈40% of the area observed by microscopic analysis and cell counts are done on multiple plains of focus. A greater number of labeled cells are observed by direct microscopy than what are shown on representative photographs.

The sensitivity of various strains of mice to lung irradiation is associated with a predisposition to the development of pulmonary inflammation (radiation pneumonitis) (24, 32, 33). C3H and C57BL6 strains of mice, in particular, develop inflammatory cell infiltrates within regions that evolve radiation-induced pathology (24). C3H and C57bl6 strains of mice, in particular, develop inflammatory cell infiltrates within regions that evolve radiation-induced pathology (24). In the present study, we found that radiation-mediated ICAM-1 expression occurred in all both of these strains mice. This finding is supported by previous studies that demonstrate inflammation in both strains (24, 32–34). Moreover, the pattern of expression was similar in each of the strains of mice in that the pulmonary capillary endothelium expressed ICAM-1, whereas the vascular endothelium from larger vessels showed no ICAM-1 expression. These data demonstrate that ICAM-1 induction may be a common event in the pathogenesis of lung injury in C3H and C57BL6 mice following thoracic irradiation.

The radiation-mediated increase in ICAM-1 mRNA expression requires no *de novo* protein synthesis and is blocked by the actinomycin D transcription inhibitor (10, 25). The 1.2-kb segment of the 5′ regulatory region of the ICAM-1 gene is sufficient to regulate activation of radiation-induced transcription (10, 25). Hallahan *et al.* (25) have also shown that binding of transcription factor NFκB to DNA is activated in endothelial cells treated with x-rays. These findings in endothelial cells are consistent with findings of NF-κB activation in irradiated lymphocytes and leukemia cell lines (35, 36). Moreover, NF-κB activation is inhibited by glucocorticoids, which are used clinically to prevent the inflammatory response to ionizing radiation.

We have previously shown that tumor necrosis factor α (TNF-α) is induced following irradiation of monocytes and human tumor cells (37, 38). IL-1 is another radiation-inducible cytokine in rodent fibroblasts (39, 40). Both TNF and IL-1 mediate inflammation by binding to their respective receptors on endothelial cells to induce the expression of the leukocyte adhesion molecules P-selectin, vascular cell adhesion molecule 1 (VCAM-1), ICAM-1, and E-selectin. We found that radiation induction of cell adhesion molecules is distinct from that observed after cytokine stimulation in that radiation induced CAMs are limited to E-selectin and ICAM, but not P-selectin or VCAM (10). Furthermore, production of TNF-α and IL-1 following irradiation of macrophages occurs 12–18 h after irradiation (37, 39), whereas E-selectin and ICAM-1 gene expression occurs 2–3 h after irradiation (25). Taken together, these data suggest that TNF-α and IL-1 are not necessary for radiation-mediated cell adhesion molecule induction in the vascular endothelium. We propose that increased cell adhesion molecule expression is essential for the pathogenesis of radiation pneumonitis and results in inflammatory changes in irradiated tissues.

Radiation therapy is a primary treatment modality for intrathoracic malignancies such as lung carcinoma, Hodgkin disease, and non-Hodgkins lymphomas involving the mediastinum. However, impaired pulmonary function following radiation therapy is a commonly observed sequela. We have found that ICAM-1 induction in the pulmonary vasculature is dose-dependent and participates in the pathogenesis of inflammatory cell infiltration of the irradiated lung. Pharmaceuticals that block ICAM-1 induction or prevent leukocyte binding to ICAM-1 may therefore reduce the incidence of lung injury following radiotherapy for intrathoracic malignancies.

We thank Yasushi Kataoka for technical assistance, Linda Degenstein (Technical Director of the University of Chicago Transgenic Core Laboratory), Dr. David Baunoch, and members of the Immunohistochemistry core laboratory. We also thank Dr. M. M. LeBeau and A. Fernald for technical assistance in developing immunofluorescent staining of lung sections. This work was funded by National Institutes of Health Grant CA58508, the American Cancer Society, the Chicago Tumor Institute, and the Center for Radiation Oncology.

1. Collins, T. (1995) *Sci. Am. Sci. Med.* **2,** 28–37.
2. Springer, T. A. (1994) *Cell* **76,** 301–314.
3. Nourshargh, S. & Williams, T. J. (1990) *J. Immunol.* **145,** 2633–2638.
4. Lo, S. K., Detmers, P. A., Levin, S. M. & Wright, S. D. (1989) *J. Exp. Med.* **169,** 1779–1793.
5. Smith, C. W., Marlin, S. D., Rothlein, R., Toman, C. & Anderson, D. C. (1989) *J. Clin. Invest.* **83,** 2008–2017.
6. Kukielka, G. (1993) *J. Clin. Invest.* **92,** 1504–1516.
7. de Fougerolles, A. R., Qin, X. & Springer, T. A. (1994) *J. Exp. Med.* **179,** 619–629.
8. Sligh, J. E. J., Ballantyne, C. M., Rich, S. S., Hawkins, H. K., Smith, C. W. & Bradley, A. (1993) *Proc. Natl. Acad. Sci. USA* **90,** 8529–8533.
9. Behrends, U., Peter, R. U., Knabe, R., Eissner, G., Holler, E., W, B. B., Caughman, S. W. & Degitz, K. (1994) *J. Invest. Dermatol.* **103,** 726–730.
10. Hallahan, D. E., Kuchibhotla, J. & Wyble, C. (1996) *Cancer Res.* **56,** 5150–5155.
11. Von Neergard, K. & Wirz, K. (1927) *Z. Clin. Med* **105,** 35–50.
12. Muhsam, R. (1904) *Arch. Klin. Chir.* **74,** 434–453.
13. Jennings, F. L. & Turner, R. A. (1961) *Arch. Pathol.* **74,** 437–446.
14. Rubin, P. & Casarett, G. W. (1968) *Clinical Radiation Pathology* (Saunders, Philadelphia).
15. Gross, N. J. (1981) *Lung* **159,** 115–125.
16. Penney, D. P. & Rubin, P. (1977) *Int. J. Radiat. Oncol. Biol. Phys.* **2,** 1123–1132.
17. Penney, D. P., Siemann, D. W., Rubin, P., Shapiro, D. L., Finkelstein, J. & Cooper, R., Jr. (1982) *Scanning Electron Micros.* **1,** 413–425.
18. Phillips, T. L. (1966) *Radiology* **87,** 49–54.
19. Steinberg, F., Quabeck, K., Rehn, B., Kraus, R., Mohnke, M., Costabel, U., Kreuzfelder, E., Molls, M., Bruch, J. & Schaefer, U. W. (1993) *Recent Results Cancer Res.* **130,** 133–143.
20. Travis, E. L., Down, J. D., Holmes, S. J. & Hobson, B. (1980) *Radiat. Res.* **84,** 133–143.
21. Travis, E. L. (1980) *Int. J. Radiat. Oncol. Biol. Phys.* **6,** 345–347.
22. Fuks, Z. (1995) *Cancer J.* **1,** 62–72.
23. Ward, H. E., Kemsley, L., Davies, L., Holecek, M. & Berend, N. (1993) *Radiat. Res.* **136,** 15–21.
24. Franko, A. J., Sharplin, J., Ghahary, A. & Barcellos-Hoff, M. H. (1997) *Radiat. Res.* **147,** 245–257.
25. Hallahan, D. E., Clark, E. T., Kuchibhotla, J., Gewertz, B. & Collins, T. (1995) *Biochem. Biophys. Res. Commun.* **217,** 784–795.
26. LeBeau, M. & Espinosa, R. (1996) *Methods in Molecular Biology* (Humana, Totowa, NJ).
27. McDonald, S., Rubin, P., Phillips, T. & Marks, L. (1995) *Int. J. Radiat. Oncol. Biol. Phys.* **31,** 1187–203.
28. Cosset, J., Socie, G., Dubray, B., Girinsky, T., Fourquet, A. & Gluckman, E. (1994) *Int. J. Radiat. Oncol. Biol. Phys.* **30,** 477–492.
29. Colden-Stanfield, M., Kalinich, J. & Gallin, E. (1994) *J. Immunol.* **153,** 5222–5229.
30. Dunn, M. M., Drab, E. A. & Rubin, D. B. (1986) *J. Appl. Physiol.* **60,** 1932–1937.
31. Hallahan, D. E., Kuchibhotla, J. & Wyble, C. (1997) *Radiat. Res.* **147,** 41–47.
32. Franko, A. J., Sharplin, J., Ward, W. F. & Hinz, J. M. (1991) *Radiat. Res.* **126,** 349–356.
33. Franko, A. J. & Sharplin, J. (1994) *Radiat. Res.* **140,** 347–355.
34. Sharplin, J. & Franko, A. J. (1989) *Radiat. Res.* **119,** 15–31.
35. Brach, M. A., Sherman, M., Gunji, H., Weichselbaum, R. R. & Kufe, D. W. (1991) *J. Clin. Invest.* **88,** 691–695.
36. Brach, M. A., Gruss, H. J., Kaisho, T., Asano, Y., Hirano, T. & Herrmann, F. (1993) *J. Biol. Chem.* **268,** 8466–8472.
37. Hallahan, D. E., Spriggs, D. R., Beckett, M. A., Kufe, D. W. & Weichselbaum, R. R. (1989) *Proc. Natl. Acad. Sci. USA* **86,** 10104–10107.
38. Sherman, M. L., Datta, R., Hallahan, D. E., Weichselbaum, R. R. & Kufe, D. W. (1991) *J. Clin. Invest.* **87,** 1794–1797.
39. O'Brien-Ladner, A., Nelson, M. E., Kimler, B. F. & Wesselius, L. J. (1993) *Radiat. Res.* **136,** 37–41.
40. Woloschak, G., Chang-Liu, C., Jones, P. & Jones, C. (1990) *Cancer Res.* **50,** 339–344.